

Concatenated Forward Error Correction with KP4 and Single Parity Check Codes

Diego Lentner, Emna Ben Yacoub, Stefano Calabrò, Georg Böcherer, Nebojša Stojanović, Gerhard Kramer

Abstract—Concatenated forward error correction is studied based on an outer KP4 Reed-Solomon code with hard-decision decoding and inner single parity check (SPC) codes with Chase/Wagner soft-decision decoding. Analytical expressions are derived for the end-to-end frame and bit error rates for transmission over additive white Gaussian noise channels with binary phase-shift keying (BPSK) and quaternary amplitude shift keying (4-ASK), as well as with symbol interleavers and quantized channel outputs. The BPSK error rates are compared to those of two other inner codes, namely a two-dimensional product code with SPC component codes and an extended Hamming code. Simulation results for unit-memory inter-symbol interference channels and 4-ASK are also presented. The results show that the coding schemes achieve similar error rates but SPC codes have the lowest complexity and permit flexible rate adaptation.

I. INTRODUCTION

APPLICATIONS such as data center networks (DCNs) and data center interconnects (DCIs) over short-reach fiber optical links have high throughput and strict latency constraints. Next-generation Ethernet standards should provide data rates of 800 Gb/s to 1.6 Tb/s [1], [2] while guaranteeing bit error rates (BERs) below 10^{-13} and latencies below 100 ns [3], [4]. Forward error correction (FEC) is essential to meet these requirements and current systems rely on the KP4 code [5], which is a $(544, 514)$ Reed-Solomon (RS) code over $\mathbb{F}_{2^{10}}$ with rate $R_{KP4} \approx 0.945$ and overhead (OH) $\approx 5.84\%$. The transition to 200 Gb/s per lane motivates improving the KP4 code by using concatenated FEC (CatFEC) [6] which has been used for medium-range links [7] where the latency constraints are less strict.

Our work is also motivated by hardware solutions where signal processing is done on pluggable or co-packaged optical modules at both ends of the optical link, and by the idea to place a low-complexity inner FEC decoder on these modules (see, e.g., [1], [3]). In this set-up, the inner decoder can access quantized channel measurements that may be used, e.g., for equalization and soft-decision decoding (SDD) of the inner code. The outer KP4 decoder is usually implemented on the Ethernet switch chip and accepts hard decisions as input.

We study CatFEC with an outer KP4 code and inner single parity check (SPC) codes. SPC codes have a simple SDD algorithm [8] and their rate can be adapted with small

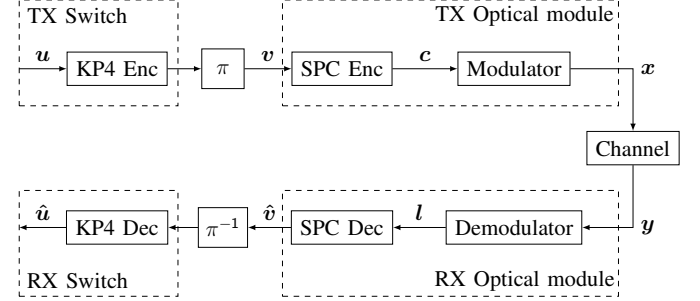


Fig. 1. CatFEC with an outer KP4 code and an inner SPC code with SDD.

granularity by varying the code length, permitting flexible rate adaptation for channels of varying qualities. In the magnetic recording literature, the paper [9] studied CatFEC with an outer RS code and inner SPC codes with SDD, and the authors provided semi-analytical methods to estimate the end-to-end error probabilities. We extend their work by deriving analytical expressions for the end-to-end frame error rates (FERs) and BERs over additive white Gaussian noise (AWGN) channels. This permits performance assessment without using numerical simulations. We compare the performance to solutions with symbol interleavers, and where the inner code is either a two-dimensional product code with SPC component codes (2D-SPC) or an extended Hamming code [10].

This paper is organized as follows. Section II introduces the proposed CatFEC scheme. In Section III, we derive analytical expressions for the end-to-end FERs and BERs with binary phase shift keying (BPSK), both without and with symbol interleavers. Sections IV and V extend the analysis to coarsely quantized inputs and to quaternary amplitude shift keying (4-ASK). Section VI compares the proposed CatFEC scheme to two alternative schemes using a 2D-SPC inner code and an extended Hamming inner code. Section VII provides simulation results for 4-ASK and a unit-memory inter-symbol interference (ISI) channel. Section VIII concludes the paper.

II. CONCATENATED SCHEME

The transceiver chain is depicted in Fig. 1. The switch chip implements an outer KP4 code that is widely deployed in current systems, and we augment the optical modules by an inner SPC code layer. We place a RS code symbol interleaver π of length $|\pi|$ between the outer and inner encoders to counteract error bursts of the inner decoder. Note that π can be implemented either on the switch integrated circuit (IC) or the optical module, or partially on both. In general, interleaving over multiple outer codewords increases the decoding latency

D. Lentner, E. Ben Yacoub, and G. Kramer are with the Institute for Communications Engineering, Technical University of Munich, 80333 Munich, Germany. E-mail: {diego.lentner, emna.ben-yacoub, gerhard.kramer}@tum.de.

S. Calabrò, G. Böcherer, and N. Stojanović are with the Huawei Munich Research Center, 80992 Munich, Germany. E-mail: {stefano.calabro, georg.bocherer, nebojsa.stojanovic}@huawei.com.

as the receiver needs to collect more code symbols before outer decoding. However, if FEC is implemented jointly over T optical lanes, interleaving over T outer codewords does not increase the system latency as compared to a *breakout* implementation with separate FEC per lane and without interleaving.

In our analysis, we therefore consider two cases:

- 1) No interleaver to model separate FEC per lane. In this case, π is the identity mapping.
- 2) A uniform block-to-block symbol interleaver¹ π to model joint FEC across multiple lanes.

We study uniform block-to-block interleavers for two reasons: to obtain analytical expressions for the error rates and because the analysis guarantees the existence of an interleaver that can achieve these error rates. We remark that convolutional interleavers [11], [12] might exhibit better latency vs. error-rate tradeoffs than block-to-block interleavers. Also, when the channel has memory the system performance can be improved by inserting a second interleaver-deinterleaver pair between the modulator/demodulator and the channel.

Let $\mathbf{u} \in \mathbb{F}_2^{k_{RS}}$, $k_{RS} = 5140$, denote the binary input to the outer KP4 RS encoder at the transmitter. After interleaving, the RS codeword's $n_{RS} = 5440$ bits are grouped into blocks $\mathbf{v} \in \mathbb{F}_2^{k_{SPC}}$ with k_{SPC} bits that are fed to the SPC encoder. The SPC encoder appends a parity bit, yielding the SPC codeword $\mathbf{c} \in \mathbb{F}_2^{n_{SPC}}$ where $n_{SPC} = k_{SPC} + 1$. Finally, suppose the signal constellation \mathcal{X} has cardinality $|\mathcal{X}| = 2^K$ where K is a positive integer. The code bits are grouped into blocks of K bits and the modulator maps these blocks to symbols $x \in \mathcal{X}$ using the inverse of the labeling function $\chi : \mathcal{X} \rightarrow \mathbb{F}_2^K$. The k -th bit of $\chi(x)$ is written as $\chi_k(x)$, $k = 1, \dots, K$.

At the receiver, the demodulator observes the channel output vector \mathbf{y} with $\lceil n_{RS}/K \rceil$ real values and converts these to the log-likelihood ratio (LLR) vector \mathbf{l} with n_{RS} real values. Each SPC codeword is then decoded individually using an SDD algorithm. In practice, multiple SPC decoders can run in parallel to lower the decoding latency. The receiver optical module passes the hard decisions $\hat{\mathbf{v}} \in \mathbb{F}_2^{k_{SPC}}$ of the systematic bits to the receiver switch module. Finally, the switch module applies deinterleaving and KP4 RS decoding to output the final estimate $\hat{\mathbf{u}} \in \mathbb{F}_2^{k_{RS}}$.

A low-complexity SDD algorithm for SPC codes is Wagner decoding [8]. This algorithm performs bitwise hard-decision decoding (HDD) with $\tilde{c}_i = \chi(\text{sgn}(l_i))$, $i = 1, \dots, n_{SPC}$, and checks if the parity check constraint is satisfied. If $\tilde{\mathbf{c}}$ is a valid SPC codeword then the decoder outputs the hard decisions of the systematic bits $\hat{\mathbf{v}} = [\tilde{c}_1 \dots \tilde{c}_{k_{SPC}}]$. Otherwise, it finds the least reliable bit (LRB) position $i' = \arg \min_i |l_i|$, flips the corresponding bit

$$\hat{\mathbf{c}} = [\tilde{c}_1 \dots \tilde{c}_{i'} \oplus 1 \dots \tilde{c}_{n_{SPC}}] \quad (1)$$

and outputs the systematic part $\hat{\mathbf{v}} = [\hat{c}_1 \dots \hat{c}_{k_{SPC}}]$. A Wagner decoder is a maximum-likelihood decoder for SPC codes over the AWGN channel [13] and is an efficient implementation of Chase decoding [14] for SPC codes. Note that Wagner decoding uses SDD only to identify the LRB, but does

¹“Uniform interleaver” refers to an interleaver that is drawn with equal probability from the set of all permutations.

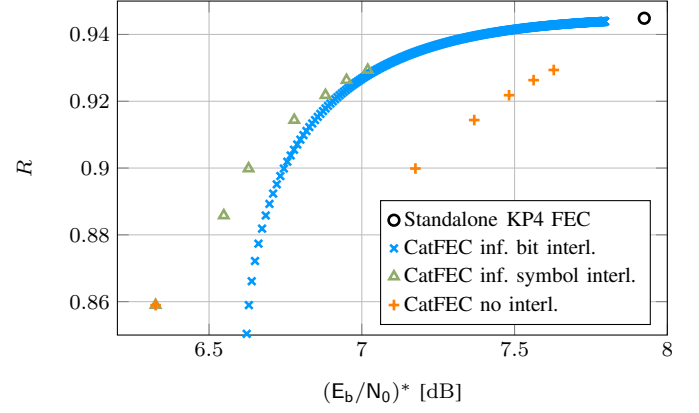


Fig. 2. CatFEC rate vs. E_b/N_0 threshold for BPSK transmission over the AWGN channel and end-to-end BER 10^{-13} .

not perform further computations, so the proposed CatFEC scheme does not require a full-precision LLR computation at the demodulator in general.

The end-to-end transmission rate of the CatFEC scheme is

$$R = R_{KP4} \cdot \frac{n_{SPC} - 1}{n_{SPC}} \cdot \log_2 |\mathcal{X}| \quad (2)$$

which can be adapted by varying n_{SPC} . Note that we do not require that $n_{SPC} - 1$ is an integer multiple of the outer RS field size, nor must $n_{SPC} - 1$ divide the outer code length.

Fig. 2 illustrates the fine granularity of rates permitted by SPC codes of different lengths. The plot is for transmission with BPSK over an AWGN channel. Let SNR^* be the signal-to-noise ratio (SNR) threshold for which the CatFEC schemes achieve the target end-to-end BER of 10^{-13} , and define $(E_b/N_0)^* = \text{SNR}^*/(2R)$. The KP4 threshold is indicated with a black circle. The blue markers show the rates for $n_{SPC} = 10, 11, 12, \dots, 1000$ for which the BER after SPC decoding meets the KP4 threshold of 3.1×10^{-4} . This BER corresponds to the target BER of 10^{-13} when the bit errors after SPC decoding are independent, but this generally requires a bit interleaver of infinite length. To compare, the red crosses in Fig. 2 show the rates without interleaving while the green triangles show the rates with an infinitely long RS symbol interleaver, in both cases for $n_{SPC} = 11, 21, \dots, 61$. Observe that a symbol interleaver performs slightly better than the bit interleaver. Also, for $n_{SPC} = 11$ the RS symbol errors after SPC decoding are independent and no interleaving performs as well as symbol interleaving. The following section gives closed-form expressions for these error rates, as well as for the error rates with symbol interleaving.

III. ERROR ANALYSIS FOR BPSK

Consider the AWGN channel with output

$$Y_j = X_j + N_j \quad (3)$$

at time j , where $X_j \in \mathcal{X}$ and $N_j \sim \mathcal{N}(0, \sigma^2)$. This section assumes BPSK with $\mathcal{X} = \{+1, -1\}$ and labeling function $\chi(+1) = 0$ and $\chi(-1) = 1$. With slight abuse of terminology, we sometimes refer to the code bits as channel inputs. By

symmetry we may assume that \mathbf{u} is the all-zeros string so the marginal probability density function of the channel output is

$$p_Y(y) = \frac{1}{\sqrt{2\pi}\sigma^2} e^{-\frac{(y-1)^2}{2\sigma^2}}. \quad (4)$$

The channel LLR $L = 2y/\sigma^2$ is Gaussian distributed with mean $\mu_{\text{ch}} = 2/\sigma^2$ and variance $\sigma_{\text{ch}}^2 = 4/\sigma^2$.

The end-to-end FER is $P_f = \Pr[\hat{\mathbf{u}} \neq \mathbf{u}]$ and the average end-to-end BER is

$$P_b = \frac{1}{k_{\text{RS}}} \sum_{i=1}^{k_{\text{RS}}} \Pr[\hat{u}_i \neq u_i]. \quad (5)$$

Define $\text{SNR} = 1/\sigma^2$ where σ^2 is the noise variance per real dimension. To measure coding gains, we plot error rates against $E_b/N_0 = \frac{\text{SNR}}{2R}$. Sometimes we plot error rates against the (uncoded) input $\text{BER}_{\text{in}} = Q(\sqrt{\text{SNR}})$, where $Q(x) = \frac{1}{\sqrt{2\pi}} \int_x^\infty e^{-\frac{a^2}{2}} da$.

A. Standalone RS Codes

Consider a (perhaps shortened) RS code of length n_{RS} and dimension k_{RS} , defined over \mathbb{F}_{2^m} , and with (bounded distance) decoding capability $t = \lfloor \frac{n_{\text{RS}} - k_{\text{RS}}}{2} \rfloor$, i.e., the decoder corrects any error pattern with t or fewer errors. For the KP4 code, we have $n_{\text{RS}} = 544$, $k_{\text{RS}} = 514$, $m = 10$, and $t = 15$. Let p denote the BER prior to RS decoding. If the transmitted bits are independent then we can express the uncoded RS symbol error probability at the channel output as $\tilde{p} = 1 - (1 - p)^m$. The output FER and symbol error probability are

$$P_{f,\text{RS}} = \sum_{i=t+1}^{n_{\text{RS}}} \binom{n_{\text{RS}}}{i} \tilde{p}^i (1 - \tilde{p})^{n_{\text{RS}}-i} \quad (6)$$

$$P_{s,\text{RS}} = \frac{1}{n_{\text{RS}}} \sum_{i=t+1}^{n_{\text{RS}}} i \binom{n_{\text{RS}}}{i} \tilde{p}^i (1 - \tilde{p})^{n_{\text{RS}}-i} \quad (7)$$

assuming that the decoder outputs the input sequence in case of failure. The average BER is

$$P_{b,\text{RS}} = \frac{p \cdot P_{s,\text{RS}}}{\tilde{p}} \quad (8)$$

which can be well-approximated as $P_{b,\text{RS}} \approx P_{s,\text{RS}}/m$ for small values of p if the decoder input bits are independent.

B. Standalone SPC Codes with Wagner Decoding

Let \mathcal{E} be the event that Wagner decoding of an SPC code fails. For $\ell = 1, \dots, n_{\text{SPC}}$, let \mathcal{A}_ℓ be the event that ℓ of the n_{SPC} hard decisions at the channel output are received in error. Moreover, let \mathcal{C}_1 be the event that there is one erroneous bit that is also the LRB, i.e., the decoder can successfully correct the only error. We have $\mathcal{E} = \{\bigcup_{\ell=1}^{n_{\text{SPC}}} \mathcal{A}_\ell\} \setminus \mathcal{C}_1$ and the FER of the SPC code is

$$P_{f,\text{SPC}} = \left(\sum_{\ell=1}^{n_{\text{SPC}}} \Pr[\mathcal{A}_\ell] \right) - \Pr[\mathcal{C}_1] \quad (9)$$

where

$$\Pr[\mathcal{A}_\ell] = \binom{n_{\text{SPC}}}{\ell} p^\ell (1 - p)^{n_{\text{SPC}}-\ell} \quad (10)$$

with $p = \text{BER}_{\text{in}} = Q(1/\sigma)$. To compute $\Pr[\mathcal{C}_1]$, by symmetry we may assume that c_1 is the LRB and write

$$\begin{aligned} \Pr[\mathcal{C}_1] &= n_{\text{SPC}} \Pr \left[\{Y_1 < 0\} \cap \left\{ \bigcap_{j=2}^{n_{\text{SPC}}} \{Y_j \geq |Y_1|\} \right\} \right] \\ &= n_{\text{SPC}} \int_{-\infty}^0 p_Y(y) Q\left(\frac{-y-1}{\sigma}\right)^{n_{\text{SPC}}-1} dy \end{aligned} \quad (11)$$

which can be easily evaluated by numerical integration.

To compute the BER $P_{b,\text{SPC}}$, we must determine how Wagner decoding affects the number of erroneous input bits. For BPSK, all code bits have the same reliability after Wagner decoding, i.e., the BER is independent of the bit position. This lets us avoid making case distinctions with respect to the parity bit that is later discarded.

Suppose now that the input to the decoder has ℓ bit errors. If ℓ is even then after decoding the codeword will still have ℓ bit errors; the probability of this event is $\Pr[\mathcal{A}_\ell]$. If ℓ is odd, we distinguish two cases: the correction event \mathcal{C}_ℓ that the LRB is among the erroneous bits, and the miscorrection event \mathcal{M}_ℓ that the LRB is not among the erroneous bits. The average BER after Wagner decoding measured with respect to the code bits or the information bits is then

$$\begin{aligned} P_{b,\text{SPC}} &= \sum_{\substack{\ell=2 \\ \ell \text{ even}}}^{n_{\text{SPC}}} \frac{\ell}{n_{\text{SPC}}} \cdot \Pr[\mathcal{A}_\ell] + \sum_{\substack{\ell=3 \\ \ell \text{ odd}}}^{n_{\text{SPC}}} \frac{\ell-1}{n_{\text{SPC}}} \cdot \Pr[\mathcal{C}_\ell] \\ &\quad + \sum_{\substack{\ell=1 \\ \ell \text{ odd}}}^{n_{\text{SPC}}-1} \frac{\ell+1}{n_{\text{SPC}}} \cdot \Pr[\mathcal{M}_\ell] \end{aligned} \quad (12)$$

where for $\ell = 1, \dots, n_{\text{SPC}}$ we have

$$\Pr[\mathcal{C}_\ell] = \binom{n_{\text{SPC}}}{\ell} \cdot \ell \cdot \int_{-\infty}^0 \phi_\ell(y) dy \quad (13)$$

$$\Pr[\mathcal{M}_\ell] = \binom{n_{\text{SPC}}}{\ell} \cdot (n_{\text{SPC}} - \ell) \cdot \int_0^\infty \psi_\ell(y) dy \quad (14)$$

with the respective

$$\phi_\ell(y) = p_Y(y) Q\left(\frac{-y+1}{\sigma}\right)^{\ell-1} Q\left(\frac{-y-1}{\sigma}\right)^{n_{\text{SPC}}-\ell} \quad (15)$$

$$\psi_\ell(y) = p_Y(y) Q\left(\frac{y+1}{\sigma}\right)^\ell Q\left(\frac{y-1}{\sigma}\right)^{n_{\text{SPC}}-\ell-1}. \quad (16)$$

Note that Wagner decoding outputs an even number of errors which is reflected in (12). Using $\Pr[\mathcal{A}_\ell] = \Pr[\mathcal{C}_\ell] + \Pr[\mathcal{M}_\ell]$ we can rewrite (12) as

$$\begin{aligned} P_{b,\text{SPC}} &= \frac{1}{n_{\text{SPC}}} \left(2 \cdot \Pr[\mathcal{M}_1] + \sum_{\ell=2}^{n_{\text{SPC}}} \ell \cdot \Pr[\mathcal{A}_\ell] \right) \\ &\quad + \sum_{\substack{\ell=3 \\ \ell \text{ odd}}}^{n_{\text{SPC}}} \frac{1}{n_{\text{SPC}}} (\Pr[\mathcal{M}_\ell] - \Pr[\mathcal{C}_\ell]) \end{aligned} \quad (17)$$

We use the exact expressions (12) or (17) for our results. As a simplification, simulations show that a good approximation and upper bound for $\text{BER}_{\text{in}} < 10^{-2}$ is

$$P_{b,\text{SPC}} \approx \frac{1}{n_{\text{SPC}}} \left(2 \cdot \Pr[\mathcal{M}_1] + \sum_{\ell=2}^{n_{\text{SPC}}} \ell \cdot \Pr[\mathcal{A}_\ell] \right). \quad (18)$$

C. Refined Analysis

We are sometimes interested in the probability that all bit errors are in one part of a codeword. Let ℓ again denote the number of erroneous code bits at the input of the SPC decoder. By symmetry, we may consider the event $\hat{\mathcal{A}}_\ell^{\kappa+1}$ that the first $n_{\text{SPC}} - \kappa - 1$ code bits are error-free *before* decoding and that all ℓ input bit errors are in the last $\kappa + 1$ code bits that include the parity bit. We compute

$$\Pr[\hat{\mathcal{A}}_\ell^{\kappa+1}] = \binom{\kappa+1}{\ell} p^\ell (1-p)^{n_{\text{SPC}}-\ell}. \quad (19)$$

Similarly, let $\hat{\mathcal{E}}_\ell^{\kappa+1}$ be the event that the first $n_{\text{SPC}} - \kappa - 1$ code bits are error-free *after* decoding, i.e., all bit errors after decoding are in the last $\kappa + 1$ bits that include the parity bit that is discarded. For even ℓ , we have $\hat{\mathcal{E}}_\ell^{\kappa+1} = \hat{\mathcal{A}}_\ell^{\kappa+1}$. For odd ℓ , we distinguish the following disjoint events:

- the correction event

$$\hat{\mathcal{C}}_\ell^{\kappa+1} = \hat{\mathcal{A}}_\ell^{\kappa+1} \cap \{\text{LRB is erroneous}\};$$

- the miscorrection event

$$\begin{aligned} \hat{\mathcal{M}}_\ell^{\kappa+1} &= \hat{\mathcal{A}}_\ell^{\kappa+1} \cap \{\text{LRB is not erroneous}\} \\ &\cap \{\text{LRB is in the last } \kappa + 1 \text{ code bits}\}; \end{aligned}$$

- the cross-miscorrection event

$$\begin{aligned} \hat{\mathcal{H}}_\ell^{\kappa+1} &= \hat{\mathcal{A}}_\ell^{\kappa+1} \cap \{\text{LRB is not erroneous}\} \\ &\cap \{\text{LRB is not in the last } \kappa + 1 \text{ code bits}\}; \end{aligned}$$

- the cross-correction event $\hat{\mathcal{K}}_\ell^{\kappa+1}$ that only $\ell - 1$ errors are in the last $\kappa + 1$ code bits before decoding, and the erroneous LRB that is corrected was in the first $n_{\text{SPC}} - \kappa - 1$ code bits.

The respective probabilities of these events are

$$\Pr[\hat{\mathcal{C}}_\ell^{\kappa+1}] = \binom{\kappa+1}{\ell} \cdot \ell \cdot \int_{-\infty}^0 \phi_\ell(y) dy \quad (20)$$

$$\Pr[\hat{\mathcal{M}}_\ell^{\kappa+1}] = \binom{\kappa+1}{\ell} \cdot (\kappa+1-\ell) \cdot \int_0^\infty \psi_\ell(y) dy \quad (21)$$

$$\Pr[\hat{\mathcal{H}}_\ell^{\kappa+1}] = \binom{\kappa+1}{\ell} \cdot (n_{\text{SPC}} - \kappa - 1) \cdot \int_0^\infty \psi_\ell(y) dy \quad (22)$$

$$\Pr[\hat{\mathcal{K}}_\ell^{\kappa+1}] = \binom{\kappa+1}{\ell-1} \cdot (n_{\text{SPC}} - \kappa - 1) \cdot \int_{-\infty}^0 \phi_\ell(y) dy. \quad (23)$$

We have $\hat{\mathcal{A}}_\ell^{\kappa+1} = \hat{\mathcal{C}}_\ell^{\kappa+1} \cup \hat{\mathcal{M}}_\ell^{\kappa+1} \cup \hat{\mathcal{H}}_\ell^{\kappa+1}$ and $\hat{\mathcal{H}}_\ell^{\kappa+1} \cap \hat{\mathcal{E}}_\ell^{\kappa+1} = \emptyset$. We also have $\hat{\mathcal{K}}_\ell^{\kappa+1} \cap \hat{\mathcal{A}}_\ell^{\kappa+1} = \emptyset$ but $\hat{\mathcal{K}}_\ell^{\kappa+1} \subseteq \hat{\mathcal{E}}_\ell^{\kappa+1}$. We thus find for odd ℓ that

$$\begin{aligned} \hat{\mathcal{E}}_\ell^{\kappa+1} &= \hat{\mathcal{K}}_\ell^{\kappa+1} \cup \{\hat{\mathcal{A}}_\ell^{\kappa+1} \setminus \hat{\mathcal{H}}_\ell^{\kappa+1}\} \\ &= \hat{\mathcal{K}}_\ell^{\kappa+1} \cup \hat{\mathcal{C}}_\ell^{\kappa+1} \cup \hat{\mathcal{M}}_\ell^{\kappa+1}. \end{aligned}$$

Note that also $\{\hat{\mathcal{K}}_\ell^{\kappa+1} \cup \hat{\mathcal{A}}_\ell^{\kappa+1}\} \subset \mathcal{A}_\ell$ since the cross-miscorrections $\hat{\mathcal{H}}_\ell^{\kappa+1}$ are not the only events that we exclude

in our constrained error rate computation. For instance, we also exclude all events where more than one of the ℓ input errors are in the first $n_{\text{SPC}} - \kappa - 1$ bits before decoding.

The constrained FER with all bit errors in the last $\kappa + 1$ code bits is then

$$\begin{aligned} \hat{\text{P}}_{\text{f,SPC}}(\kappa) &= \sum_{\substack{\ell=2 \\ \ell \text{ even}}}^{\kappa+1} \Pr[\hat{\mathcal{A}}_\ell^{\kappa+1}] + \sum_{\substack{\ell=3 \\ \ell \text{ odd}}}^{\kappa+1} \Pr[\hat{\mathcal{C}}_\ell^{\kappa+1}] \\ &\quad + \sum_{\substack{\ell=3 \\ \ell \text{ odd}}}^{\kappa+2} \Pr[\hat{\mathcal{K}}_\ell^{\kappa+1}] + \sum_{\substack{\ell=1 \\ \ell \text{ odd}}}^{\kappa} \Pr[\hat{\mathcal{M}}_\ell^{\kappa+1}] \end{aligned} \quad (24)$$

Unlike in (9), the constrained BER on the systematic bits differs from the constrained BER over the entire codeword, as the parity bit that is discarded may be erroneous. We therefore compute the the constrained systematic BER $\hat{\text{P}}_{\text{b,SPC}}(\kappa)$ as

$$\begin{aligned} \frac{\frac{\kappa}{\kappa+1}}{k_{\text{SPC}}} &\left(\sum_{\substack{\ell=2 \\ \ell \text{ even}}}^{\kappa+1} \ell \cdot \Pr[\hat{\mathcal{A}}_\ell^{\kappa+1}] + \sum_{\substack{\ell=3 \\ \ell \text{ odd}}}^{\kappa+1} (\ell-1) \cdot \Pr[\hat{\mathcal{C}}_\ell^{\kappa+1}] \right. \\ &\quad \left. + \sum_{\substack{\ell=3 \\ \ell \text{ odd}}}^{\kappa+2} (\ell-1) \cdot \Pr[\hat{\mathcal{K}}_\ell^{\kappa+1}] + \sum_{\substack{\ell=1 \\ \ell \text{ odd}}}^{\kappa} (\ell+1) \cdot \Pr[\hat{\mathcal{M}}_\ell^{\kappa+1}] \right) \end{aligned} \quad (25)$$

where the factor $\frac{\kappa}{\kappa+1}$ accounts for the fraction of bit errors in the systematic bits only. Note that $\hat{\text{P}}_{\text{b,SPC}}(k_{\text{SPC}}) = \text{P}_{\text{f,SPC}}$, i.e., (25) reduces to (12) if we allow all code bits to be erroneous since $\hat{\mathcal{K}}_\ell^{\kappa+1} = \emptyset$ and $\hat{\mathcal{H}}_\ell^{\kappa+1} = \emptyset$ for all ℓ .

D. Error Rates Without Interleaver

Suppose there is no interleaver between the outer and inner codes and let $\text{LCM}(x, y)$ be the least common multiple of x and y . The inner SPC decoder causes burst errors across $\tau = \text{LCM}(k_{\text{SPC}}, m)/m$ outer RS code symbols. If τ divides n_{RS} then each RS codeword can be partitioned into $n_\tau = \frac{n_{\text{RS}}}{\tau}$ blocks of τ RS symbols that we study separately. For $i = 0, \dots, \tau$, let P_i be the probability that exactly i RS symbols of the τ -tuple are in error prior to outer decoding, and let z_i be the total number of such τ -tuples with i erroneous symbols within one RS codeword. We have $\sum_{i=0}^\tau P_i = 1$, $\sum_{i=0}^\tau z_i = n_\tau$, and the end-to-end FER

$$\text{P}_{\text{f}} = \sum_{\substack{z_0, \dots, z_\tau \geq 0 \\ \sum_{i=0}^\tau z_i = n_\tau \\ \sum_{i=1}^\tau i \cdot z_i \geq t+1}} \binom{n_\tau}{z_0, \dots, z_\tau} \prod_{i=0}^\tau P_i^{z_i}. \quad (26)$$

Furthermore, let $P_{b,i}$ be the BER due to τ -tuples with i symbol errors prior to outer decoding such that $\sum_{i=1}^\tau P_{b,i} = \text{P}_{\text{b,SPC}}$. The CatFEC BER is then

$$\text{P}_{\text{b}} = \sum_{\substack{z_0, \dots, z_\tau \geq 0 \\ \sum_{i=0}^\tau z_i = n_\tau \\ \sum_{i=1}^\tau i \cdot z_i \geq t+1}} \left(\frac{\sum_{i=1}^\tau z_i \frac{P_{b,i}}{P_i}}{n_\tau} \right) \binom{n_\tau}{z_0, \dots, z_\tau} \prod_{i=0}^\tau P_i^{z_i}. \quad (27)$$

Note that for $\tau = 1$, (26) and (27) are equivalent to the basic RS error probability expressions (6)–(8) with $\tilde{p} = P_1$ and $p = P_{b,1}$.

Example 1 (KP4 & inner (11,10) SPC codes). We have $k_{\text{SPC}} = m$, i.e., each SPC covers exactly one outer RS symbol, which yields the aforementioned case where $\tau = 1$ and $n_\tau = n_{\text{RS}} = 544$. The FER and BER of the CatFEC scheme are directly obtained by inserting $P_1 = P_{f,\text{SPC}}$ and $P_{b,1} = P_{b,\text{SPC}}$ into (26) and (27).

Example 2 (KP4 & inner (6,5) SPC codes). We again have $\tau = 1$ and $n_\tau = n_{\text{RS}} = 544$ since each outer RS symbol is protected by exactly two SPC codes. This time, however, $P_1 = 1 - (1 - P_{f,\text{SPC}})^2$ and $P_{b,1} = P_{b,\text{SPC}}$.

Example 3 (KP4 & inner (21,20) SPC codes). We have $\tau = 2$ and $n_\tau = n_{\text{RS}}/2 = 272$, i.e., always two RS symbols are coupled by one inner SPC code. The probability that the first RS symbol is error-free and the second symbol is erroneous is $\hat{P}_{f,\text{SPC}}(10)$, and vice versa. We thus find $P_1 = 2 \cdot \hat{P}_{f,\text{SPC}}(10)$ and $P_2 = P_{f,\text{SPC}} - P_1$. Likewise, $P_{b,1} = 2 \cdot \hat{P}_{b,\text{SPC}}(10)$ and $P_{b,2} = P_{b,\text{SPC}} - P_{b,1}$.

Example 4 (KP4 & inner $(\tau m + 1, \tau m)$ SPC codes). In this more general case, one SPC codeword matches exactly τ RS symbols. Let P'_i , $i = 1, \dots, \tau$, be the probability that all the first i RS symbols of one τ -tuple are erroneous and the remaining $\tau - i$ symbols are error-free. We have the recursion $P'_i = \hat{P}_{f,\text{SPC}}(im) - \sum_{j=1}^{i-1} \binom{i}{j} P'_j$ and compute $P_i = \binom{\tau}{i} P'_i$. Analogously, we have $P'_{b,i} = \hat{P}_{b,\text{SPC}}(im) - \sum_{j=1}^{i-1} \binom{i}{j} P'_{b,j}$ and $P_{b,i} = \binom{\tau}{i} P'_{b,i}$.

If n_{RS} does not divide τ then we must additionally consider the correlations between consecutive outer codewords to compute the exact error probabilities. We adopt another approach where we set $n_\tau = \lceil \frac{n_{\text{RS}}}{\tau} \rceil$, for which (26) becomes an upper bound and for which (27) holds only approximately. However, simulation results show that for $n_{\text{RS}} \gg \tau$, both the FER and BER are accurately predicted by this approach.

Example 5 (KP4 & inner (16,15) SPC codes). We have $\tau = 3$ since three RS symbols are covered by two SPC codes. Since n_{RS} is not an integer multiple of $\tau = 3$, we have $n_\tau = \lceil \frac{n_{\text{RS}}}{\tau} \rceil = 182$. Numerical results show that (26) and (27) accurately predict the end-to-end FER and BER for low error rates.

E. Error Rates with Uniform Symbol Interleaver

Suppose now there is a uniform interleaver π that randomly permutes the $|\pi| = T \cdot n_{\text{RS}}$ RS symbols of T outer RS codewords. Clearly, if $T = 1$ then the error probabilities remain the same as without an interleaver since the error correction capability of the outer RS code does not depend on the positions of the erroneous symbols.

At the other extreme, in the limit $|\pi| \rightarrow \infty$, the symbol errors become uncorrelated after inner decoding and deinterleaving. To compute the symbol error probability after the deinterleaver, we must consider their bursty nature before interleaving. More precisely, the average symbol error rate and

the average BERs after inner decoding and prior to deinterleaving are $\bar{P} = \frac{1}{\tau} \sum_{i=1}^{\tau} i P_i$ and $\bar{P}_b = \sum_{i=1}^{\tau} P_{b,i} = P_{b,\text{SPC}}$, respectively. The end-to-end FERs and BERs of the interleaved CatFEC scheme are then directly obtained by inserting $\tilde{p} = \bar{P}$ and $p = \bar{P}_b$ into (6)–(8).

For small T , as required by low-latency applications, the above asymptotic analysis is not precise enough. Instead, by carefully considering the correlations among the symbol errors at each stage of decoding, we can express the FERs and BERs in closed form for the interleaved set-up. For $i = 0, \dots, \tau$, let z_i be the total number of τ -tuples with i erroneous symbols within the T outer codewords after inner Wagner decoding, and prior to deinterleaving and decoding. The probability that the T outer codewords contain in total $e = \sum_{i=1}^{\tau} i \cdot z_i$ individual symbol errors is then

$$P(e) = \sum_{\substack{z_0, \dots, z_\tau \geq 0 \\ \sum_{i=0}^{\tau} z_i = T \cdot n_\tau \\ \sum_{i=1}^{\tau} i \cdot z_i = e}} \binom{T \cdot n_\tau}{z_0, \dots, z_\tau} \prod_{i=0}^{\tau} P_i^{z_i}. \quad (28)$$

The deinterleaver π^{-1} distributes the e symbol errors uniformly over the T outer codewords but does not change e itself. For $i = 0, \dots, T$, the joint probability that codeword i will contain $0 \leq e_i \leq n_{\text{RS}}$ symbol errors after deinterleaving is given by the multivariate hypergeometric distribution

$$g(e_0, \dots, e_T) = \frac{\prod_{i=1}^T \binom{n_{\text{RS}}}{e_i}}{\binom{T n_{\text{RS}}}{e}} \quad (29)$$

with $e = \sum_{i=1}^T e_i$. This can be seen by considering the (de)interleaving as a sampling without replacement: Consider an urn with $T \cdot n_{\text{RS}}$ balls of T different colors, with n_{RS} balls of each color. Suppose the balls from each color are labeled with numbers from one to n_{RS} . Each color represents one outer codeword, and the balls their position within this codeword. By drawing e balls we select the symbol error positions after deinterleaving. The probability to pick e_i balls from color i , $i = 1, \dots, T$ is then given by (29).

RS (bounded distance) decoding of the i -th codeword will succeed if $e_i \leq t$, and fail if $e_i > t$. The overall end-to-end FER of the interleaved CatFEC scheme is then

$$P_f = \sum_{e_0, \dots, e_T \geq 0} \frac{\sum_{i=1}^T \epsilon(e_i)}{T} \cdot g(e_0, \dots, e_T) \cdot P \left(\sum_{i=0}^T e_i \right) \quad (30)$$

where $\epsilon(e_i) = 0$ if $e_i \leq t$ and $\epsilon(e_i) = 1$ if $e_i > t$. Similarly, we derive the end-to-end BER as

$$P_b = \sum_{e_0, \dots, e_T \geq 0} \frac{\sum_{i=1}^T e_i \cdot \epsilon(e_i)}{T \cdot n_{\text{RS}}} \cdot g(e_0, \dots, e_T) \cdot P_b \left(\sum_{i=0}^T e_i \right) \quad (31)$$

where $P_b(e)$ is

$$\sum_{\substack{z_0, \dots, z_\tau \geq 0 \\ \sum_{i=0}^{\tau} z_i = T \cdot n_\tau \\ \sum_{i=1}^{\tau} i \cdot z_i = e}} \left(\frac{\sum_{i=1}^{\tau} z_i \frac{P_{b,i}}{P_i}}{\frac{T \cdot n_\tau}{P_i}} \right) \cdot \binom{T \cdot n_\tau}{z_0, \dots, z_\tau} \prod_{i=0}^{\tau} P_i^{z_i}. \quad (32)$$

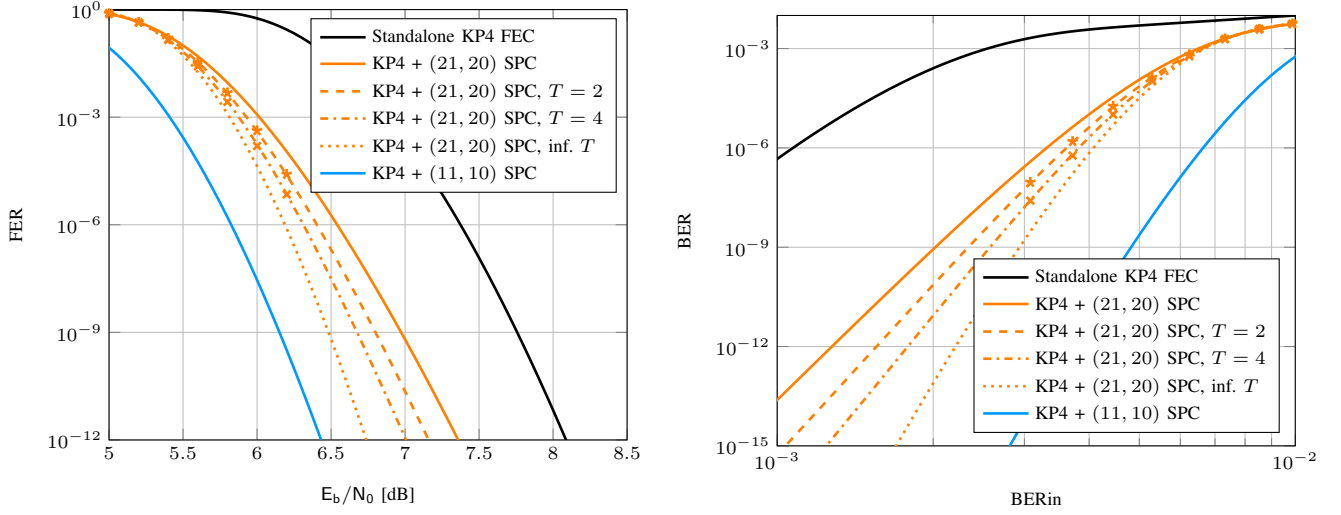


Fig. 3. End-to-end FERs (left) and BERs (right) for BPSK transmission over the AWGN channel, with and without interleaving between an outer KP4 code and an inner SPC code of lengths $n_{\text{SPC}} = 11, 21$.

Note that if $T \cdot n_{\text{RS}}$ does not divide τ then we can use the same trick as at the end of Sec. III-D and set $T \cdot n_{\text{RS}} = \lceil \frac{T \cdot n_{\text{RS}}}{\tau} \rceil$ to compute (28) and (32). As before, (28) and (30) are now upper bounds and (31) and (32) are approximations. As long as $T \cdot n_{\text{RS}} \gg \tau$, both P_f and P_b are closely approximated by (30) and (31), respectively.

Fig. 3 plots the FER P_f and BER P_b with and without interleaving for the codes from Examples 1 and 5. The FER and BER of a standalone KP4 code are plotted in black as a benchmark. For $n_{\text{SPC}} = 11$, we have $\tau = 1$, i.e., all symbol errors are uncorrelated prior to outer decoding even without an interleaver. The FER and BER therefore remain the same in both cases and are shown by the blue solid line. For $n_{\text{SPC}} = 21$, we show the error probabilities without an interleaver (orange solid), with uniform interleavers of lengths $T = 2$ (orange dashed) and $T = 4$ (orange dash-dotted), and an infinitely long uniform interleaver (orange dotted). We see that $T = 4$ suffices to achieve half of the asymptotic E_b/N_0 interleaving gain at $\text{FER} = 10^{-12}$. The orange markers depict simulation results for $n_{\text{SPC}} = 21$ and $T = 2, 4$, and for a fixed interleaver realization. As can be seen, the analysis not only describes the average ensemble performance, but also accurately predicts the FER and BER for specified (typical) interleaver realizations.

IV. QUANTIZED CHANNEL OUTPUTS

We extend the above analysis to coarsely quantized soft channel outputs. Consider a uniform b -bit quantizer with transfer function

$$f_{\Delta}(x) = \text{sign}(x) \cdot \Delta \cdot \min \left\{ 2^{b-1} - \frac{1}{2}, \left\lfloor \frac{|x|}{\Delta} \right\rfloor + \frac{1}{2} \right\} \quad (33)$$

where the quantization step Δ should be optimized. An input $x \in \mathbb{R}$ is quantized to $\lambda_i = (i - \frac{1}{2})\Delta$, $i = -2^{b-1} + 1, \dots, 2^{b-1}$

if $g_{i-1} \leq x \leq g_i$, where

$$g_i = \begin{cases} -\infty, & i = -2^{b-1} \\ i\Delta, & -2^{b-1} < i < 2^{b-1} \\ +\infty, & i = 2^{b-1}. \end{cases} \quad (34)$$

We derive the FER for $k_{\text{SPC}} = m$ where each RS symbol is protected by a single SPC codeword.

Let $\bar{L} = f_{\Delta}(L)$ denote the channel LLR after quantization which is distributed as

$$p_{\bar{L}}(\lambda_i) = Q\left(\frac{g_{i-1} - \mu_{\text{ch}}}{\sigma_{\text{ch}}}\right) - Q\left(\frac{g_i - \mu_{\text{ch}}}{\sigma_{\text{ch}}}\right) \quad (35)$$

for $i = -2^{b-1} + 1, \dots, 2^{b-1}$. Apart from dealing with discrete LLRs, we must now consider the event of multiple LRBs with equal reliability $|\bar{L}|$. In this case, the Wagner decoder picks one of the LRBs uniformly at random and flips it if the parity check is not satisfied. Suppose there is only one erroneous bit with quantized LLR $\bar{l} = \lambda_i$, $i \in \{-2^{b-1} + 1, \dots, 0\}$, which is also an LRB. Furthermore, let there be another z LRBs with the same reliability but that are correct, i.e., with quantized LLR $-\bar{l} = \lambda_{-i+1}$. This occurs with probability

$$\varphi_z(i) = p_{\bar{L}}(\lambda_i) p_{\bar{L}}(\lambda_{-i+1})^z \left(\sum_{j=-i+2}^{2^{b-1}} p_{\bar{L}}(\lambda_j) \right)^{n_{\text{SPC}}-z-1}. \quad (36)$$

There are $\binom{n_{\text{SPC}}}{z+1}$ possibilities to arrange the $z+1$ LRBs, and the probability to pick and correct the erroneous bit is $\frac{1}{z+1}$. Thus, the overall probability that a single bit error is corrected by the Wagner decoder is

$$\Pr[\mathcal{C}_1] = \sum_{i=-2^{b-1}+1}^0 \sum_{z=0}^{n_{\text{SPC}}-1} \binom{n_{\text{SPC}}}{z+1} \frac{1}{z+1} \varphi_z(i). \quad (37)$$

Inserting (10) and (37) into (9) yields the SPC FER $P_{f,\text{SPC}}$. The end-to-end FER of the CatFEC scheme follows from (26) and $P_1 = P_{f,\text{SPC}}$.

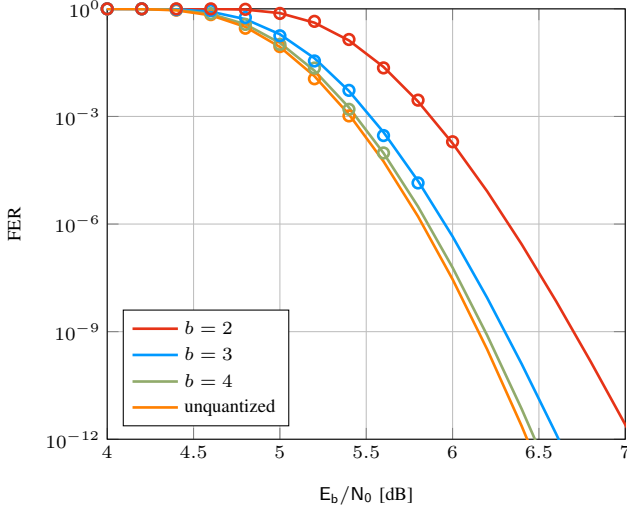


Fig. 4. End-to-end FERs with inner (11,10) SPC code for BPSK transmission over the AWGN channel when the channel output is quantized to $b = 2, 3, 4$ bits.

Fig. 4 plots the FER of our CatFEC scheme with an outer KP4 code and an inner SPC code of length $n_{\text{SPC}} = 11$ when the channel output is quantized with $b = 2$ (—), $b = 3$ (—), and $b = 4$ (—) bits, respectively, and for an unquantized channel output (—). Again, the solid lines show the analytical error probabilities and the markers depict the corresponding end-to-end FERs of numerical simulations. Observe that $b = 3$ bits resolution gives close-to-optimal performance even for low error rates.

V. EXTENSION TO 4-ASK

The analysis extends to higher-order modulation and bit-metric decoding (BMD) by considering the different reliabilities at each bit level. We derive the FER of 4-ASK where $X_j \in \mathcal{X} = \{\pm 3\delta, \pm\delta\}$ where δ satisfies $\mathbb{E}[X^2] = 1$. For simplicity we consider $k_{\text{SPC}} = m$ so that $\tau = 1$.

We have $K = 2$ and define $B_k = \chi_k(X)$, $k = 1, 2$, for a generic 4-ASK input X . The LLRs for the corresponding channel output $Y = y$ are

$$l_k = \log \frac{P_{B_k|Y}(0|y)}{P_{B_k|Y}(1|y)}, \quad k = 1, 2 \quad (38)$$

where uppercase letters (such as Y) denote random variables and lowercase letters (such as y) denote realizations. If the channel LLRs L_k fulfill the symmetry constraint

$$p_{L_k|B_k}(l|0) = p_{L_k|B_k}(-l|1), \quad l \in \mathbb{R}, \quad k = 1, 2 \quad (39)$$

then we may assume that an all-zeros codeword was transmitted. However, the bit channels $p_{L_k|B_k}$ are generally not symmetric.

To introduce symmetrized counterparts for 4-ASK, we use *channel adapters* [15] that apply a pseudo-random binary scrambling string at both the transmitter and receiver. As a result, L_k is replaced with

$$\tilde{L}_k = L_k \cdot (1 - 2B_k) \quad (40)$$

and the bit-channels $p_{\tilde{L}_k|B_k}$ are symmetric since

$$p_{\tilde{L}_k|B_k}(l|0) = p_{\tilde{L}_k|B_k}(-l|1). \quad (41)$$

We further use *surrogate channels* [16]–[19] and approximate $p_{\tilde{L}_k|B_k}$ by an AWGN channels with uniform binary inputs for which the deriving the cumulative distribution functions (CDFs) simplifies. We require that the true channel and its surrogate have the same channel uncertainty. Let the surrogate be $\check{Y}_k = \check{X}_k + \check{N}_k$ with $\check{X}_k \in \{-1, +1\}$ and $\check{N}_k \sim \mathcal{N}(0, \check{\sigma}_k^2)$ for $k = 1, 2$. We calculate for each SNR the set of equivalent channel parameters

$$\check{\sigma}_k^2 : H(\check{B}_k|\check{Y}) = H(B_k|Y), \quad k = 1, 2 \quad (42)$$

where $H(X|Y)$ is the average entropy of X given Y . Under the Gaussian approximation, the LLRs \tilde{L}_k are Gaussian with mean $\check{\mu}_{\text{ch},k} = \frac{2}{\check{\sigma}_k^2}$ and variance $\check{\sigma}_{\text{ch},k}^2 = \frac{4}{\check{\sigma}_k^2}$, and the hard-decision BER is $p_k = Q\left(\frac{\check{\mu}_{\text{ch},k}}{\check{\sigma}_{\text{ch},k}}\right)$ for $k = 1, 2$.

Suppose that N_1 code bits of an SPC codeword are mapped to bit level B_1 , and that the other $N_2 = n_{\text{SPC}} - N_1$ code bits are mapped to bit level B_2 . The SPC FER after Wagner decoding is

$$P_{\text{f,SPC}}(N_1, N_2) = \sum_{\substack{0 \leq \ell_1 \leq N_1 \\ 0 \leq \ell_2 \leq N_2 \\ \ell_1 + \ell_2 \geq 1}} \Pr[\mathcal{A}_{\ell_1, \ell_2}] - \Pr[\mathcal{C}_1] \quad (43)$$

where

$$\Pr[\mathcal{A}_{\ell_1, \ell_2}] = \prod_{k=1}^2 \binom{N_k}{\ell_k} p_k^{\ell_k} (1 - p_k)^{N_k - \ell_k} \quad (44)$$

$$\Pr[\mathcal{C}_1] = \sum_{k=1}^2 N_k \int_{-\infty}^0 \phi_k(a) da \quad (45)$$

with

$$\phi_1(a) = p_{\tilde{L}_1}(a) Q\left(\frac{-a - \check{\mu}_{\text{ch},1}}{\check{\sigma}_{\text{ch},1}}\right)^{N_1-1} Q\left(\frac{-a - \check{\mu}_{\text{ch},2}}{\check{\sigma}_{\text{ch},2}}\right)^{N_2} \quad (46)$$

$$\phi_2(a) = p_{\tilde{L}_2}(a) Q\left(\frac{-a - \check{\mu}_{\text{ch},1}}{\check{\sigma}_{\text{ch},1}}\right)^{N_1} Q\left(\frac{-a - \check{\mu}_{\text{ch},2}}{\check{\sigma}_{\text{ch},2}}\right)^{N_2-1}. \quad (47)$$

We assume that the SPC code bits are alternately mapped to the two bit levels B_1 and B_2 , respectively. This leads to correlated SPC frame errors and, since $\tau = 1$, also to correlated RS symbol errors of length $\tau' = \frac{\text{LCM}(n_{\text{SPC}}, 2)}{2}$, respectively. For all $i = 0, \dots, \tau'$, let P_i be the probability that exactly i RS symbols of the τ' -tuple are in error prior to outer decoding, and let z_i be the total number of such τ' -tuples with i erroneous symbols within one RS codeword. Clearly, we have $\sum_{i=0}^{\tau'} P_i = 1$ and $\sum_{i=0}^{\tau'} z_i = n_{\tau'}$.

For example, for an outer KP4 code we have $n_{\text{SPC}} = m + 1 = 11$, $\tau' = 2$ and $n_{\tau'} = n_{\text{RS}}/2$. The FERs of the two SPC codewords within one 2-tuple are

$$P_{\text{f,SPC}_1} = P_{\text{f,SPC}}(\lceil \frac{n_{\text{SPC}}}{2} \rceil, \lfloor \frac{n_{\text{SPC}}}{2} \rfloor) \quad (48)$$

$$P_{\text{f,SPC}_2} = P_{\text{f,SPC}}(\lfloor \frac{n_{\text{SPC}}}{2} \rfloor, \lceil \frac{n_{\text{SPC}}}{2} \rceil) \quad (49)$$

yielding

$$P_1 = (1 - P_{\text{f,SPC}_1})P_{\text{f,SPC}_2} + P_{\text{f,SPC}_1}(1 - P_{\text{f,SPC}_2}) \quad (50)$$

$$P_2 = P_{\text{f,SPC}_1}P_{\text{f,SPC}_2}. \quad (51)$$

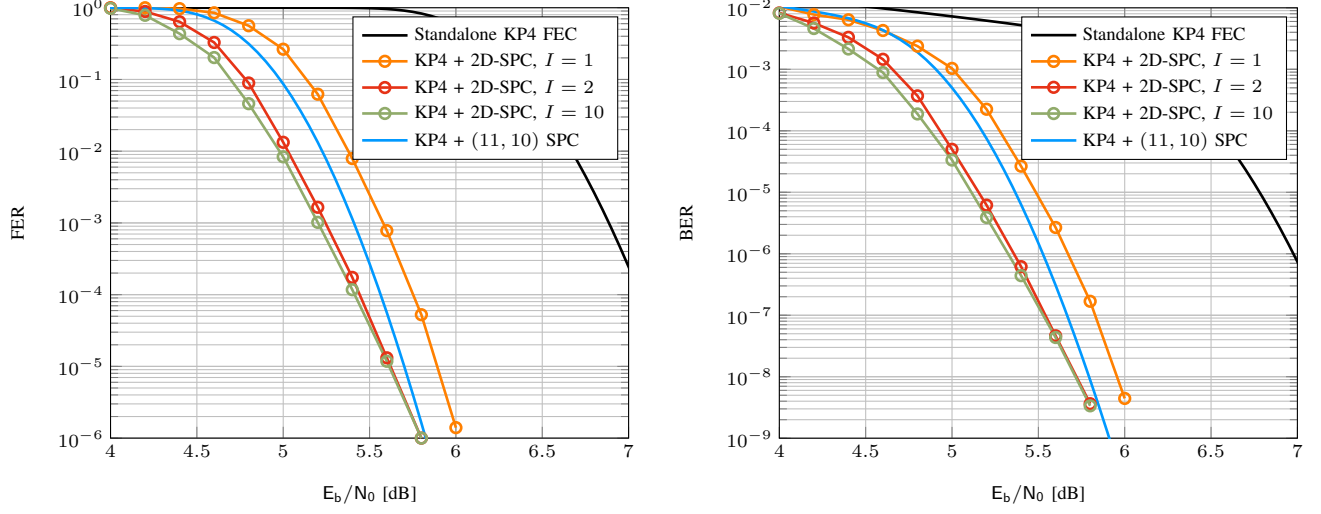


Fig. 5. End-to-end FERs (left) and BERs (right) of a CatFEC scheme with an outer KP4 code and a) an inner $(21^2, 20^2)$ 2D-SPC code with soft product decoding, b) an inner $(11, 10)$ SPC code and Wagner decoding. The plots were generated for BPSK transmission over the AWGN channel without interleaving.

The overall end-to-end FER of the CatFEC scheme is thus

$$P_f = \sum_{\substack{z_0, \dots, z_{\tau'} \geq 0 \\ \sum_{i=0}^{\tau'} z_i = n_{\tau'} \\ \sum_{i=1}^{\tau'} i \cdot z_i \geq t+1}} \binom{n_{\tau'}}{z_0, \dots, z_{\tau'}} \prod_{i=0}^{\tau'} P_i^{z_i}. \quad (52)$$

Alternatively, one could use multilevel coding (MLC) [20], [21] where each bit level is protected by a separate SPC code. This leads again to $n_{\tau'} = n_{RS}/2$ independent 2-tuples of RS symbols that are mapped to the two bit levels B_1 and B_2 , respectively. The end-to-end FER of the CatFEC scheme with MLC and BMD is then obtained by inserting $P_{f,SPC1} = P_{f,SPC}(n_{SPC}, 0)$ and $P_{f,SPC2} = P_{f,SPC}(0, n_{SPC})$ into (50)–(52). In a more general setting, SPC codes of different lengths can be used for each bit level, giving another degree of freedom to optimize the CatFEC system.

VI. COMPARISON TO ALTERNATIVE SCHEMES

Consider BPSK transmission over the AWGN channel. We compare the performance of our CatFEC scheme to two alternative CatFEC schemes where the inner SPC code is replaced by a 2D-SPC code or a $(128, 120)$ extended Hamming code. We again apply a soft-in, hard-out inner decoder, and use the KP4 outer code.

For both schemes, performance is evaluated by Monte Carlo simulations. When we can compute the FER and BER analytically, we plot the error probabilities in solid lines without markers. Simulation results are plotted with markers. We adjust the length of the inner SPC code to obtain the (approximately) same end-to-end rate as each alternative CatFEC scheme. We assume separate FEC per optical lane and therefore no interleaving for all simulations.

A. Inner $(441, 400)$ 2D-SPC Code

Consider a two-dimensional product code with $(21, 20)$ SPC component codes, i.e., the inner code parameters are

$(21^2, 20^2)$. The rate of this 2D-SPC code is 0.9070 and the end-to-end transmission rate is $R = 0.8570$, which corresponds to an overall FEC OH of 16.68%. We compare to the proposed CatFEC scheme with an inner $(11, 10)$ SPC code where the end-to-end transmission rate is $R = 0.8590$ (16.42% OH). We apply soft product decoding with bitwise maximum a posteriori (MAP) decoding of the component SPC codes and with hard decisions after I full iterations.

The FER and BER of the 2D-SPC code is depicted in Fig. 5 for $I = 1, 2, 10$ decoding iterations. Note that $I = 2$ achieves almost the full coding gain for FERs below 10^{-5} . This observation agrees with [22] where the performance of n -dimensional SPC product codes converges after n decoding iterations. Next, the FER slope of the CatFEC scheme with the inner 2D-SPC and soft product decoding is smaller than that of the proposed CatFEC scheme. While at $FER = 10^{-2}$ the former code gains approximately 0.25 dB over latter code, the FER curves of both schemes intersect at $FER \approx 10^{-6}$, making the inner SPC code preferable for low error rates. Both effects are also observed for the BERs.

B. Inner $(128, 120)$ Extended Hamming code

Consider now the $(128, 120)$ extended Hamming code as an inner code. The end-to-end transmission rate of the concatenated system is $R = 0.8858$ (12.89% OH). We compare this CatFEC scheme to the proposed scheme with the $(16, 15)$ SPC code of same rate as the Hamming code.

The Hamming code is decoded with a Chase decoder [14, Alg. 2] with 2^ν test patterns, where ν is the number of LRB positions used to form the test list. Given the input LLRs \mathbf{l} , the Chase decoder first computes the hard decisions $\mathbf{d} = \chi(\text{sgn}(\mathbf{l}))$ and reliability values $\mathbf{r} = |\mathbf{l}|$, where both the sign and absolute value are taken element-wise. Based on \mathbf{r} , the decoder identifies the positions of the ν LRBs and forms a test list \mathcal{T}_ν by making 2^ν copies of the vector \mathbf{d} and replacing the ν LRBs by all binary combinations of length ν . We call

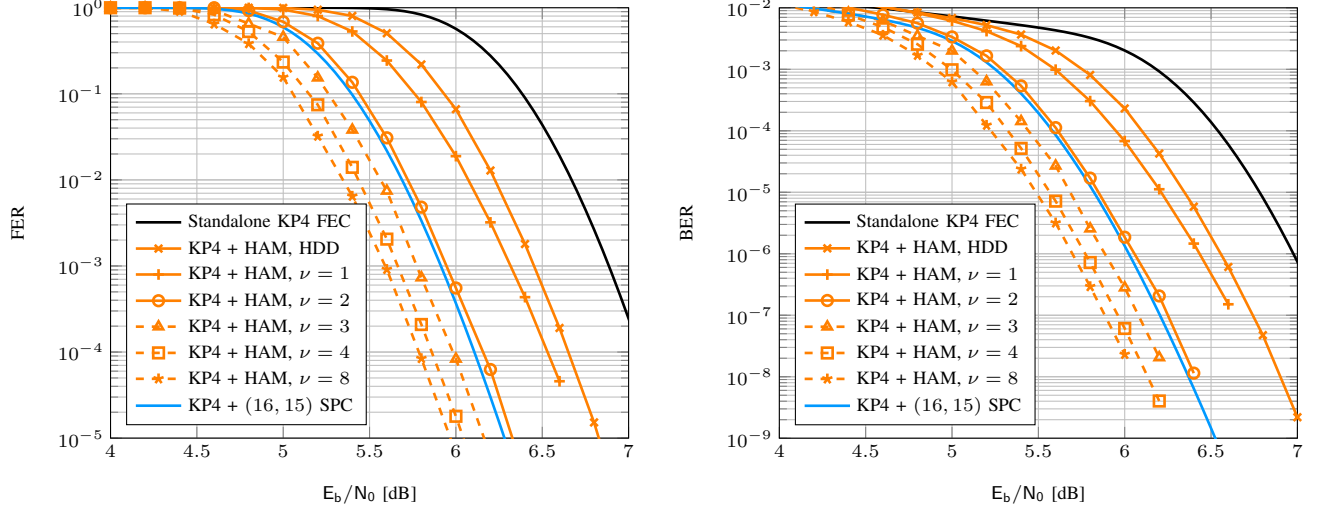


Fig. 6. End-to-end FERs (left) and BERs (right) of a CatFEC scheme with an outer KP4 code and a) an inner (128, 120) Hamming code with Chase decoding, b) an inner (16, 15) SPC code and Wagner decoding. The plots were generated for BPSK transmission over the AWGN channel without interleaving.

each member $z \in \mathcal{T}_\nu$ of the list a test word, and the vector $t = d \oplus z$ the corresponding test pattern. For each test word z in the test list, one bounded distance decoding (BDD) attempt is performed. The decoder returns the binary error vector e (with respect to z) if successful, otherwise it flags a decoding failure. For each successful BDD attempt, the Chase decoder computes the *analog weight* as the inner product

$$w = \sum_{i=1}^n \tilde{e}_i r_i \quad (53)$$

of the combined error vector $\tilde{e} = t \oplus e$. The Chase decoder keeps track of the combined error vector \tilde{e}^* of lowest analog weight w^* and outputs $\hat{c} = d \oplus \tilde{e}^*$.

Chase decoding as in [14, Alg. 2] guarantees correcting up to $d - 1$ errors for a code with minimum distance d by considering only the $\nu = \lfloor \frac{d}{2} \rfloor$ LRBs. The performance improves by choosing larger values of ν . Since the minimum distance of the extended Hamming code is $d = 4$, we have $\nu = \lfloor \frac{d}{2} \rfloor = 2$, i.e., $2^{\lfloor \frac{d}{2} \rfloor} = 4$ test patterns. However, we also study larger test list sizes to illustrate the potential gains.

C. Decoding Complexity

We quantify the complexity by the number of elementary operations required to decode one codeword, i.e., the number of logical XOR and AND operations as well as the number of additions of two reals. We omit counting the number of pairwise comparisons of reals, as this number depends on the sorting algorithm. For example, Wagner decoding of an SPC code of length n_{SPC} is particularly simple: $n_{\text{SPC}} - 1$ bitwise XOR operations for the syndrome computation and one XOR to potentially flip the LRB.

The complexity of Chase decoding a (n_H, k_H) Hamming code depends on the number ν of LRBs used to generate the test list. For each of the 2^ν test words, we need to compute the syndrome and the analog weight of the combined error vector. We assume a syndrome-based look-up table (LUT)

TABLE I
NUMBER OF ELEMENTARY OPERATIONS REQUIRED FOR A) WAGNER DECODING OF EIGHT (16, 15) SPC CODEWORDS, B) CHASE DECODING OF ONE (128, 120) HAMMING CODEWORD WITH $\nu = 1, 2, 3, 4, 8$.

	XORs	ANDs	real ADDs
8 \times SPC(16,15)	128	—	—
HAM(128,120), HDD	1144	1024	—
HAM(128,120), $\nu = 1$	2416	2048	254
HAM(128,120), $\nu = 2$	4704	4096	508
HAM(128,120), $\nu = 3$	9280	8192	1016
HAM(128,120), $\nu = 4$	18432	16384	2032
HAM(128,120), $\nu = 8$	292992	262144	32512

implementation of BDD and neglect the complexity of the look-up operation. The binary syndrome vector is computed by multiplying with the parity-check matrix of dimension $(n_H - k_H) \times n_H$, which in general would require up to $(n_H - k_H)n_H$ AND and $(n_H - k_H)(n_H - 1)$ XOR operations. Each analog weight calculation requires n_H XOR operations to determine the combined error vector \tilde{e} , as well as $n_H - 1$ real additions for the inner product (53). Note that this inner product computation does not require real multiplications since the elements of \tilde{e} are either zero or one. The final computation of \hat{c} requires n_H more XOR operations.

In contrast, HDD of the Hamming code requires $(n_H - k_H)n_H$ AND and $(n_H - k_H)(n_H - 1)$ XOR operations for syndrome computation, and another n_H XOR operations for adding the error vector from the LUT to the input. Note that simply setting $\nu = 0$ in the above complexity calculations would yield a larger complexity score since some steps like the computation of \tilde{e} and (53) are not required for HDD.

To make the comparison as fair as possible, we compute the complexity of decoding the same number of code bits (or, equivalently, the same number of information bits). Table I shows the complexity to decode 8 codewords of the (16, 15) SPC code and 1 codeword of the (128, 120) Hamming code. Observe that even in the case of HDD the Hamming code

requires one order of magnitude more logical operations than Wagner decoding of the SPC codes. For $\nu = 2$, the complexity is almost two orders of magnitude larger than Wagner decoding of the SPC codewords. For larger ν , the Hamming decoder can become prohibitively complex.

Fig. 6 shows the end-to-end FERs (left) and BERs (right) of the CatFEC schemes for BPSK modulation and transmission over the AWGN channel. Remarkably, the inner (16, 15) SPC code slightly outperforms the Hamming code in both FER and BER even when $\nu = \lfloor \frac{d}{2} \rfloor = 2$. Compared to HDD the inner Hamming code, the SPC code exhibits a coding gain of approximately 0.5 dB. Chase decoding with $\nu > 2$ lets the Hamming code improve on the SPC code but at the cost of substantial decoding complexity.

VII. UNIT-MEMORY ISI CHANNELS

A common channel model in optical communications is the time-discrete, unit-memory ISI channel

$$Y_j = X_j + \alpha X_{j-1} + N_j \quad (54)$$

with interference level $0 \leq \alpha \leq 1$ and white Gaussian noise $N_j \sim \mathcal{N}(0, \sigma^2)$ per real dimension. The unit-memory ISI channel models the effective channel after applying linear minimum mean squared error (LMMSE) filtering and noise whitening. In this section, we consider 4-ASK modulation with Gray labelling [23] and normalized transmit power $\mathbb{E}[X^2] = 1$. By means of Monte Carlo simulations, we study the performances of the CatFEC schemes presented in Sec. VI when applied to the 4-ASK ISI channel.

As before, we plot the error rates against $E_b/N_0 = \frac{\text{SNR}}{2R}$, where R is the end-to-end transmission rate, and where the SNR is redefined as $\text{SNR} = \frac{1+\alpha^2}{\sigma^2}$. We use the consecutive bit-to-symbol mapping as described in Sec. V with BMD at the receiver. Given a channel output vector \mathbf{y} , the demapper computes the bit-wise posterior LLRs in two steps:

- 1) Compute the symbol-wise posterior probabilities $P_{X_j|\mathbf{Y}}(x|\mathbf{y})$ using the forward-backward algorithm [24].
- 2) Compute the posterior LLR of the k -th bit $\chi_k(X_j)$ of the j -th channel input symbol X_j via marginalization:

$$l_{j,k} = \log_2 \frac{\sum_{\tilde{x} \in \mathcal{X} : \chi_k(\tilde{x})=0} P_{X_j|\mathbf{Y}}(\tilde{x}|\mathbf{y})}{\sum_{\tilde{x} \in \mathcal{X} : \chi_k(\tilde{x})=1} P_{X_j|\mathbf{Y}}(\tilde{x}|\mathbf{y})}. \quad (55)$$

Consider again the two codes from Section VI-A. Fig. 7 shows the FER and BER performances for interference levels $\alpha = 0, 0.2, 0.4, 0.6, 0.8$ (from left to right), respectively. The error rates for the CatFEC scheme with inner $(21^2, 20^2)$ 2D-SPC code and $I = 2$ soft product iterations are depicted by solid orange lines. The solid blue lines show the error rates for the CatFEC scheme with inner (11, 10) SPC code and Wagner decoding.

Consider first $\alpha = 0$ (circles), i.e., 4-ASK transmission over the interference-free AWGN channel. As in the BPSK case, observe that the 2D-SPC code has a small advantage over the (11,10) SPC code at high FERs. However, the slope for the (11,10) SPC code is larger, which suggests that this code

performs better at lower error rates. As α increases to 0.6, the gap between the curves for the 2D-SPC and the (11,10) SPC increases slightly. Interestingly, the gap reduces again as α is further increased to 0.8. Again, all effects can be observed for both the FERs and BERs.

The performance of the two codes from Sec. VI-B behaves similarly. Fig. 8 shows the FER and BER for interference levels $\alpha = 0, 0.2, 0.4, 0.6, 0.8$ (from left to right), respectively. The error rates of the CatFEC scheme with inner (128, 120) Hamming code and Chase decoding with $\nu = 2$ are depicted with solid orange lines. The solid blue lines show the error rates for the CatFEC scheme with inner (16, 15) SPC code and Wagner decoding.

For $\alpha = 0$, the results are consistent with their BPSK counterparts. The SPC code has a small advantage over the more complex Hamming code, which becomes slightly larger as the interference level increases. We see that that relative performance of the codes is similar to the BPSK+AWGN model, which shows that this model is a reasonable proxy to design codes for the 4-ASK ISI channel. The analysis in Sec. III is thus useful to evaluate the performance in the target error rate regime without computation-heavy simulations, even when using finite-length interleavers.

We conclude with two remarks. First, in the presence of ISI, the performance of all presented CatFEC schemes can be further improved by using a channel interleaver, see Sec. II. We expect that the much shorter SPC codes require much shorter channel interleavers than, e.g., the (128,120) Hamming code. Second, there is potential to reduce the computational complexity of Step 1) of the LLR computation (forward-backward algorithm) when using SPC codes as inner codes since we do not require the soft information to be true LLRs.

VIII. CONCLUSION

We investigated FEC codes for short-reach optical links with strict latency requirements. We proposed a CatFEC scheme based on an outer KP4 FEC and soft-decoded inner SPC codes and provided analytical expressions for the end-to-end FER and BER of the concatenated system both without and with RS symbol interleavers. Numerical results show that SPC codes as inner codes are competitive with CatFEC schemes with more sophisticated inner codes even when operated at the “sweet spot” of the latter codes, while having considerably lower decoding complexity. The relative coding gains for BPSK transmission over the AWGN channel and for 4-ASK signaling over an ISI channel with AWGN remained approximately constant, which justifies using the former as a proxy for code design for the latter.

REFERENCES

- [1] J. D’Ambrosia, K. Lusted, G. Nicholl, D. Ofelt, M. Nowell, M. Brown, and R. Stone, “Project overview—IEEE P802.3df: 200 Gb/s, 400 Gb/s, 800 Gb/s, and 1.6 Tb/s Ethernet,” IEEE 802.3 Beyond 400 Gb/s Ethernet Study Group, Tech. Rep., Oct. 2021. [Online]. Available: https://grouper.ieee.org/groups/802/3/B400G/public/21_1028/B400G_overview_c_211028.pdf
- [2] 800 Gigabit Ethernet (GbE) Specification, Ethernet Technology Consortium Std., Rev. 1.1, Jun. 2021. [Online]. Available: https://ethernettechnologyconsortium.org/wp-content/uploads/2021/10/Ethernet-Technology-Consortium_800G-Specification_r1.1.pdf

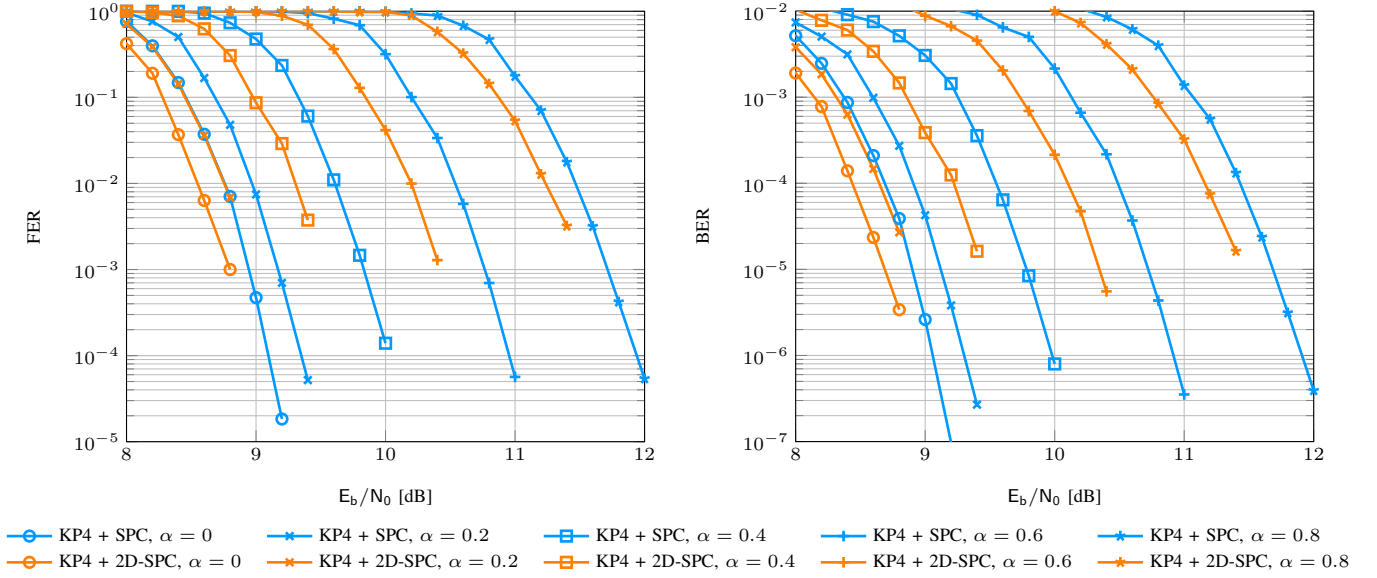


Fig. 7. End-to-end FERs (left) and BERs (right) of CatFEC schemes with an inner (11, 10) SPC code and an inner (441, 400) 2D-SPC code ($I = 2$). The FERs and BERs are shown for the unit-memory ISI channel with 4-ASK modulation and interference levels $\alpha = 0, 0.2, 0.4, 0.6, 0.8$, and without interleavers.

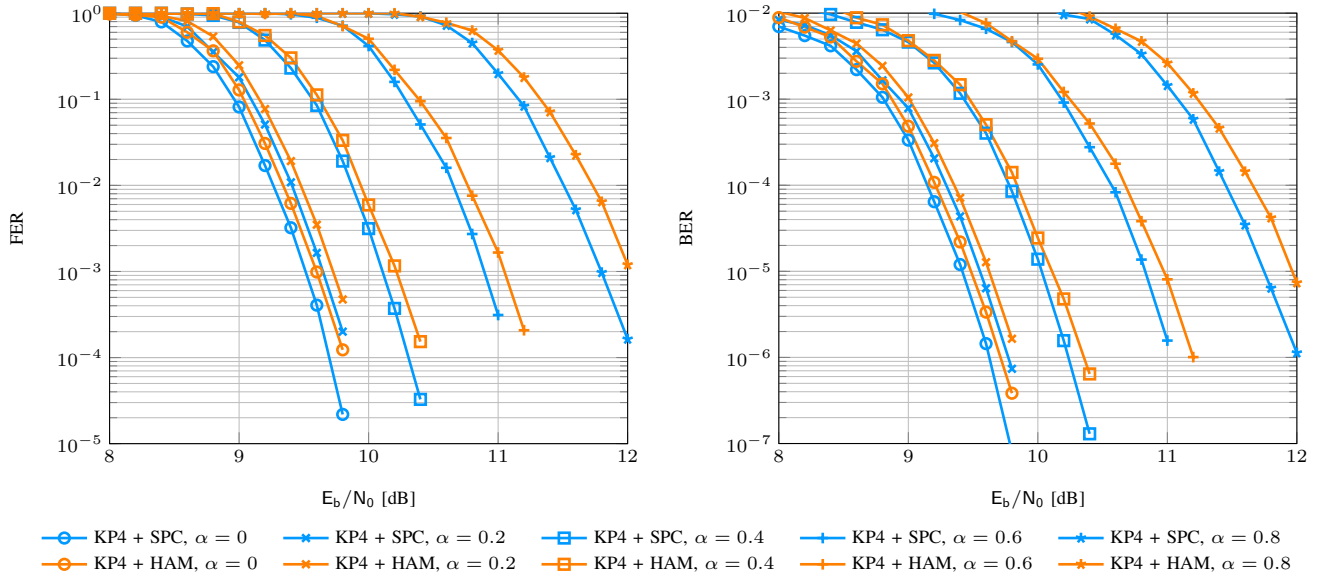


Fig. 8. End-to-end FERs (left) and BERs (right) of CatFEC schemes with an inner (16, 15) SPC code and an inner (128, 120) Hamming code ($\nu = 2$). The FERs and BERs are shown for the unit-memory ISI channel with 4-ASK modulation and interference levels $\alpha = 0, 0.2, 0.4, 0.6, 0.8$, and without interleavers.

- [3] X. He, H. Ren, and X. Wang, "FEC architecture of B400GbE to support BER objective," IEEE 802.3 Beyond 400 Gb/s Ethernet Study Group, Tech. Rep., May 2021. [Online]. Available: https://grouper.ieee.org/groups/802/3/B400G/public/21_05/he_b400g_01_210426.pdf
- [4] J. D'Ambrosia, "Objectives," IEEE P802.3df 200 Gb/s, 400 Gb/s, 800 Gb/s, and 1.6 Tb/s Ethernet Task Force, Tech. Rep., Mar. 2022. [Online]. Available: https://www.ieee802.org/3/df/proj_doc/objectives_P802d3df_220317.pdf
- [5] IEEE Standard for Ethernet, IEEE Std. 802.3-2018 (Revision of IEEE Std. 802.3-2015), Aug. 2018. [Online]. Available: <https://doi.org/10.1109/IEEESTD.2018.8457469>
- [6] D. Forney, "Concatenated codes," Sc.D. thesis, Massachusetts Institute of Technology, 1965.
- [7] Implementation Agreement 400ZR, Optical Internetworking Forum (OIF) Std. OIF-400ZR-01.0, Mar. 2020. [Online]. Available: https://www.oiforum.com/wp-content/uploads/OIF-400ZR-01.0_reduced2.pdf
- [8] R. Silverman and M. Balser, "Coding for constant-data-rate systems," *IRE Trans. Inf. Theory*, vol. PGIT-4, pp. 50–63, Sep. 1954.
- [9] P. Chaichanavong and G. Burd, "On the concatenation of soft inner code with Reed–Solomon code for perpendicular magnetic recording," *IEEE Trans. Magn.*, vol. 43, no. 2, pp. 744–749, 2007.
- [10] A. Nedelcu, S. Calabrò, Y. Lin, and N. Stojanović, "Concatenated SD-Hamming and KP4 codes in DCN PAM4 4x200 Gbps/lane," in *Proc. Eur. Conf. Optical Commun. (ECOC)*, Basel, Switzerland, Sep. 2022, pp. (We.3.C.6) 1–4.
- [11] J. Ramsey, "Realization of optimum interleavers," *IEEE Trans. Inf. Theory*, vol. 16, no. 3, pp. 338–345, May 1970.
- [12] G. Forney, "Burst-correcting codes for the classic bursty channel," *IEEE Trans. Commun. Technol.*, vol. 19, no. 5, pp. 772–781, Oct. 1971.
- [13] J. Wolf, "Efficient maximum likelihood decoding of linear block codes using a trellis," *IEEE Trans. Inf. Theory*, vol. 24, no. 1, pp. 76–80, Jan. 1978.
- [14] D. Chase, "Class of algorithms for decoding block codes with channel measurement information," *IEEE Trans. Inf. Theory*, vol. 18, no. 1, pp.

- 170–182, Jan. 1972.
- [15] J. Hou, P. H. Siegel, L. B. Milstein, and H. D. Pfister, “Capacity-approaching bandwidth-efficient coded modulation schemes based on low-density parity-check codes,” *IEEE Trans. Inf. Theory*, vol. 49, no. 9, pp. 2141–2155, Sep. 2003.
 - [16] F. Peng, W. Ryan, and R. Wesel, “Surrogate-channel design of universal LDPC codes,” *IEEE Commun. Lett.*, vol. 10, no. 6, pp. 480–482, Jun. 2006.
 - [17] M. Franceschini, G. Ferrari, and R. Raheli, “Does the performance of LDPC codes depend on the channel?” *IEEE Trans. Commun.*, vol. 54, no. 12, pp. 2129–2132, Dec. 2006.
 - [18] I. Sason, “On universal properties of capacity-approaching LDPC code ensembles,” *IEEE Trans. Inf. Theory*, vol. 55, no. 7, pp. 2956–2990, Jul. 2009.
 - [19] F. Steiner, G. Böcherer, and G. Liva, “Protograph-based LDPC code design for shaped bit-metric decoding,” *IEEE J. Sel. Areas Commun.*, vol. 34, no. 2, pp. 397–407, Feb. 2016.
 - [20] H. Imai and S. Hirakawa, “A new multilevel coding method using error-correcting codes,” *IEEE Trans. Inf. Theory*, vol. 23, no. 3, pp. 371–377, May 1977.
 - [21] U. Wachsmann, R. F. Fischer, and J. B. Huber, “Multilevel codes: Theoretical concepts and practical design rules,” *IEEE Trans. Inf. Theory*, vol. 45, no. 5, pp. 1361–1391, Jul. 1999.
 - [22] D. Rankin and T. Gulliver, “Single parity check product codes,” *IEEE Trans. Commun.*, vol. 49, no. 8, pp. 1354–1362, Aug. 2001.
 - [23] F. Gray, “Pulse code communication,” U.S. Patent 2 632 058, Mar. 17, 1953.
 - [24] L. Bahl, J. Cocke, F. Jelinek, and J. Raviv, “Optimal decoding of linear codes for minimizing symbol error rate,” *IEEE Trans. Inf. Theory*, vol. 20, no. 2, pp. 284–287, Mar. 1974.